Two splice variants of Golgi-microtubule-associated protein of 210 kDa (GMAP-210) differ in their binding to the *cis*-Golgi network

Francisco RAMOS-MORALES*, Carmen VIME*, Michel BORNENS†, Concepción FEDRIANI* and Rosa M. RIOS*[1]

*Departamento de Microbiología, Facultad de Biología, Universidad de Sevilla, Apdo. 1095, 41080 Sevilla, Spain, and †Institut Curie, Section Recherche, UMR144 du CNRS, 75248 Paris, Cedex 05, France

GMAP-210 (Golgi-microtubule-associated protein of 210 kDa) is a peripheral Golgi protein that interacts with the minus end of microtubules through its C-terminus and with *cis*-Golgi network membranes through its N-terminus; it participates in the maintenance of the structural integrity of the Golgi apparatus [Infante, Ramos-Morales, Fedriani, Bornens and Rios (1999) J. Cell Biol. **145**, 83–98]. We report here the cloning of a new isoform of GMAP-210 that lacks amino acid residues 105–196. On the basis of the analysis of the *gmap-210* genomic sequence, we propose that the small isoform, GMAP-200, arises from alternative splicing of exon 4 of the primary transcript. Overexpression of GMAP-200 induces perturbations in both the Golgi apparatus and the microtubule network that are similar to those previously reported for GMAP-210 overexpression. We show that both isoforms are able to oligomerize under overexpression conditions. Analysis *in vitro* and *in vivo*, with the green fluorescent protein as a marker, reveals that the binding of the N-terminal domain of GMAP-200 to the *cis*-Golgi network membranes is lower than that of the N-terminal domain of GMAP-210. Implications for the regulation of interaction between the *cis*-Golgi network and microtubules are discussed.

Key words: gene organization, isoform, membrane binding, microtubules.

INTRODUCTION

Interaction of the Golgi complex with cytoskeletal elements, particularly microtubules, is required for maintaining the characteristic spatial localization of the Golgi apparatus within cells and for the efficient delivery of proteins and lipids to diverse cellular sites. In higher eukaryotic cells, the Golgi complex is centred on the centrosome and is actively maintained there. This is an optimal localization for enabling transport intermediates derived from the endoplasmic reticulum to use radially arranged microtubules converging at one central localization. Membrane flux out of the Golgi complex to plasma membrane or back to the endoplasmic reticulum is also facilitated by microtubules. A major focus of current work in this area has been to clarify the role of molecular motors in regulating the balance of membrane inflow and outflow pathways that underlie the subcellular distribution and size of the Golgi complex (reviewed in [1,2]). It has been reported that the Golgi apparatus, as many other organelles, remains attached to microtubules when motor function is inactivated [3–5], indicating that there exists a class of molecules that binds the organelle statically to microtubules. We have recently characterized one such protein, GMAP-210 (Golgi-microtubule-associated protein of 210 kDa), that links membranes of the *cis*-Golgi network (CGN) to the minus end of microtubules [6].

GMAP-210 was initially described as a peripheral Golgi autoantigen of 210 kDa whose localization was restricted to the CGN. This protein exhibited an unusual behaviour when cells were treated with nocodazole or Brefeldin A. Nocodazole induced a specific and early segregation of many GMAP-210-associated vesicles or tubules from the Golgi apparatus. On treatment with Brefeldin A, GMAP-210 did not redistribute in the endoplasmic reticulum but exhibited a vesicular pattern characteristic of proteins residing in the CGN [7]. The full-length cDNA encoding GMAP-210 predicts a protein of 1979 amino acid residues with a three-domain structure consisting of two non-helical end domains separated by a long α-helical domain with high potential to form a coiled-coil structure. The presence of a very long coil encompassing most of the sequence and the analysis of heptad repeats support the possibility of a dimeric form for GMAP-210 *in vivo*. Deletion analyses *in vitro* showed that the N-terminus binds to Golgi membranes, whereas the C-terminus binds to the ends of microtubules. Consistently, when transfected in fusion with the green fluorescent protein (GFP), the N-terminal domain associated with the CGN, whereas the C-terminal microtubule-binding domain was localized at the centrosome. Overexpression of GMAP-210-encoding cDNA induced a marked enlargement and partial fragmentation of the Golgi apparatus. The microtubule network in the centrosomal area also seemed modified: instead of the microtubule aster, a dense network of short microtubules was visible at the centrosome. These effects did not occur when a truncated form lacking the C-terminal domain was expressed, indicating that perturbation of the Golgi apparatus is primarily due to an excess of binding to microtubules. Taken together, these results support the view that GMAP-210 serves to link the CGN to the minus ends of centrosome-nucleated microtubules and uncover a critical role for this interaction in ensuring the proper localization and size of the Golgi apparatus [6].

Here we report the cloning of a cDNA coding for a new isoform of GMAP-210 lacking residues 105–196. Analysis of the *gmap-210* genomic sequence revealed that residues 105–196 correspond exactly to exon 4, suggesting that this isoform, which we have called GMAP-200, arises from alternative splicing of the primary transcript. GMAP-200 is expressed in HeLa and COS-7 cells as detected by reverse-transcriptase-mediated PCR (RT–PCR) and Western blotting and seems to have a lower binding capacity for Golgi membranes. On the basis of these differences we discuss a possible role in regulating the association between the CGN and microtubules in the pericentrosomal area.

Abbreviations used: CGN, *cis*-Golgi network; GFP, green fluorescent protein; HA, haemagglutinin; GST, glutathione S-transferase; RT–PCR, reverse-transcriptase-mediated PCR.

[1] To whom correspondence should be addressed (e-mail rmrios@cica.es).

EXPERIMENTAL

Molecular cloning and sequencing of GMAP-200

Recombinants (10^6) of a λZAPII human HeLa cell random-primed cDNA expression library (P. Chambon, Strasbourg, France) were screened with serum from a patient with Sjögren syndrome, as described [6]. pBluescript phagemids containing the cloned cDNA inserts were excised from λZAPII by co-infection with R408 helper phage as described in the manufacturer's instructions (Stratagene). DNA isolation from transformed bacteria and recombinant DNA manipulations were performed by standard procedures [8]. A series of overlapping restriction fragments from the clones obtained by immuno-screening were subcloned into pBluescript SK or pTZ19R. Double-stranded cDNA in pBluescript or pTZ19R was sequenced on both strands with an automatic sequencer (Pharmacia) by the dideoxy termination method. Sequence data were compiled and analysed with the University of Wisconsin Genetics Computer Group package version 8.1 for Unix computers and the EGCG extensions to the Wisconsin package, version 8.1.0.

To obtain a haemagglutinin (HA) epitope-tagged GMAP-200 protein [9], the fragment obtained by PCR with primers P5 (5′-GTC AGA ATT CTA TGT CGT CCT GGC TTG GGG GC-3′) and P8 (5′-GTC ACT CGA GCG GCA TCA GAC AGT GCT TGT TG-3′) was used to replace the equivalent fragment in pECE-HA-GMAP-210 [6]. Partial GMAP-210 or GMAP-200 cDNA species were also cloned into the prokaryotic expression plasmid pGEX4T-2. Finally, whole GMAP-210 cDNA and cDNA fragments coding for residues 1–375 of GMAP-210 (ΔC375) or 1–283 of GMAP-200 (ΔC283) were cloned in fusion with GFP into the eukaryotic expression vector pEGFP-N1.

Preparation of glutathione S-transferase (GST) fusion proteins

The synthesis of the GST fusion proteins was induced by the addition of 1 mM isopropyl β-D-thiogalactoside to bacteria containing the plasmids pGEX4T-2/R2 or pGEX4T-2/Rs1. The fusion proteins were isolated from bacterial lysates by affinity chromatography with glutathione–agarose beads (Sigma).

RT–PCR amplification

HeLa mRNA was prepared with a Quick Prep mRNA purification kit (Pharmacia Biotech). First-strand cDNA synthesis was performed with an oligo(dT) primer by using a First-strand cDNA synthesis kit (Pharmacia Biotech). The completed first-strand reaction was amplified directly by PCR with specific primers P7 (5′-CGG AAT TCT GGG CAG CCT GGC TTC CCT C-3′) and P6 (5′-TAA TTC TTC TCG ATG TCG TCG-3′).

Cell culture and lysis

HeLa and COS-7 cells were grown in Dulbecco's modified Eagle's medium supplemented with 10 % (v/v) foetal calf serum, 2 mM L-glutamine, 100 i.u./ml penicillin and 100 μg/ml streptomycin. Cells were maintained in a humidified air/CO_2 (19:1) atmosphere at 37 °C. For cell lysis, cells were washed and harvested in PBS. Cells (2×10^7 to 10^8/ml) were lysed at 4 °C in NP40 buffer [10 mM Tris/HCl (pH 7.4)/150 mM NaCl/10 % (v/v) glycerol/1 % (v/v) Nonidet P40/1 mM PMSF/1 μg/ml pepstatin/1 μg/ml leupeptin/1 μg/ml aprotinin] for 20 min. The extract was centrifuged at 20000 ***g*** for 20 min and both supernatant (soluble fraction) and pellet (insoluble fraction) were stored at −70 °C.

Antibodies

Serum (designated RM) from a patient with Sjögren syndrome was divided into aliquots; after the addition of NaN_3 it was stored at −70 °C. The IgG fraction (10 mg/ml final concentration) was purified from whole serum on Protein A–Sepharose columns and stored in 50 % (v/v) glycerol at −70 °C. Specific antibodies from serum RM were affinity-purified on nitrocellulose strips with immunoreactive proteins from total cell extracts, as described in [10]. Anti-(GMAP-210) polyclonal antibody RM130 was generated in rabbits by using GST fusion proteins containing residues 375–611 and 618–803 from GMAP-210, as described [6]. CTR433 is a medial Golgi marker [11]. Anti-giantin monoclonal antibody [12] was a gift from H. P. Hauri (Switzerland). Anti-HA monoclonal antibody was from Boehringer Mannheim (Indianapolis, IN, U.S.A.). Anti-GFP monoclonal antibody was from ClonTech. Anti-IgG secondary antibodies were from Promega or Amersham.

Electrophoresis and immunoblot analyses

Proteins were separated by SDS/PAGE and gels were stained with Coomassie Brilliant Blue. Non-stained gels were transferred electrophoretically to nitrocellulose filters that were blocked for 1 h at 37 °C in TBST [10 mM Tris/HCl (pH 7.4)/150 mM NaCl/0.1 % (v/v) Tween 20] containing 5 % (w/v) non-fat dried milk. Filters were then incubated for 1–2 h at 37 °C in the primary antibody diluted in TBST containing 5 % non-fat dried milk, washed in the same buffer and incubated for 45 min at 37 °C with secondary anti-rabbit, anti-mouse or anti-human IgG antibodies conjugated with peroxidase (Amersham). After washes with TBST, peroxidase activity was revealed with the ECL® system (Amersham).

Transient transfection

Plasmid DNA used for transfection was purified through two preparative CsCl/ethidium bromide equilibrium gradients, followed by extraction with phenol and precipitation with ethanol. COS-7 cells were split 24 h before transfection so that they were 60–80 % confluent on the day of transfection. Cells [($2–5 \times 10^6$ per assay] were resuspended in 200 μl of serum-containing medium buffered with 15 mM Hepes, mixed with 50 μl of 210 mM NaCl containing 5–40 μg of plasmid DNA and electroporated with a Bio-Rad Gene Pulser. At 6 h after electroporation, medium was replaced by fresh medium and cells were processed after 24–48 h.

Co-immunoprecipitation experiments

COS-7 cells were transfected with 20 μg of either pEGFP-GMAP-210, pECE-HA-GMAP-200 or both and, after 24 h, lysed in NP40 buffer as described previously. For co-immunoprecipitation experiments, soluble fractions of singly and doubly transfected cells were preadsorbed with 10 μl of an irrelevant serum on 50 μl of Protein A–Sepharose and then immunoprecipitated with 10 μl of anti-HA antibody on 50 μl of Protein A–Sepharose. After incubation and washing, beads pellets were analysed by Western blotting with anti-GFP, anti-HA or RM130 antibodies.

Subcellular fractionation

COS-7 cells transfected with 20 μg of pEGFP-Δ375 or pEGFP-Δ283 were harvested 24 h after transfection and homogenized in 50 mM Tris/HCl (pH 7.5)/1 mM EDTA/150 mM NaCl/0.25 M sucrose/1 mM PMSF/1 μg/ml pepstatin/1 μg/ml leupeptin/

1 μg/ml aprotinin by repetitive passage through a 26-gauge hypodermic needle attached to a 1 ml insulin syringe. The homogenate was centrifuged at 2000 ***g*** for 20 min at 4 °C. The supernatant was further centrifuged at 100000 ***g*** for 30 min at 4 °C to precipitate membrane fractions. Equal proportions of all fractions were subjected to SDS/PAGE [8 % (w/v) gel] and analysed by immunoblotting as described.

Immunofluorescence microscopy

Indirect immunofluorescence was performed as described [7]. For GFP fluorescence, cells were fixed in 4 % (w/v) paraformaldehyde and permeabilized in acetone at −30 °C for 3 min. Epifluorescence microscopy was performed with a Leica microscope.

RESULTS

We screened 10^6 recombinant phages carrying cDNA from human HeLa cells with the autoimmune serum RM, from a patient with Sjögren syndrome [6]. During this screening, which led to the cloning of *gmap-210* cDNA, we identified five independent clones coding for the 5′ end of the cDNA. A restriction map of these clones, termed R1, R2, R3, Rs1 and Rs2, revealed that a fragment of approx. 0.3 kb containing a *Pst*I restriction site was absent from Rs1 and Rs2 clones. A comparison of the restriction patterns of R2, Rs1 and Rs2 clones is shown in Figure 1(A). An internal fragment of clone R2 (nt 357–1488 of *gmap-210*) and the corresponding sequence in Rs1 were cloned into pGEX bacterial expression vectors. GST-fusion polypeptides were produced in bacteria, subjected to electrophoresis, blotted and probed with the autoimmune serum. As shown in Figure 1(B), both GST–R2 and GST–Rs1 were recognized by the serum, confirming the specificity of the immunological screening. Analysis of the sequences of the five clones obtained showed that they were identical except for a 276 bp deletion in Rs1 and Rs2 that corresponded to nt 669–944 in the *gmap-210* cDNA sequence (accession number Y12490; Figure 1C). This deletion does not alter the reading frame in the mRNA but results in a protein 92 residues shorter than the originally described GMAP-210. Isolation of two independent clones carrying the same deletion suggests that two isoforms of GMAP-210 are expressed in HeLa cells.

To ascertain whether a short variant of *gmap-210* could exist in the cells, RT–PCR was performed on mRNA isolated from HeLa cells by using primers P7 and P6, corresponding to nt 416–434 in the upper strand and 1110–1130 in the lower strand respectively (Figure 2A). The two main bands obtained had approximate sizes of 0.7 and 0.4 kb (Figure 2B), which correlated with the expected bands for the long and the short forms of *gmap-210* mRNA. To show the specificity of the bands they were purified and reamplified with the same primers (Figure 2C) and were digested with *Pst*I and *Bcl*I restriction enzymes (Figure 2D). *Pst*I cut the long form into three bands, two of identical sizes (approx. 320 bp) and a third of 60 bp (not seen in the gel), whereas the short form was cut into only two bands of 340 and 60 bp. As expected, both forms were digested at the same position by *Bcl*I, generating a band of 150 bp (not seen in the gel) and a band 150 bp smaller than the non-digested bands. These results show that the restriction patterns of two bands obtained by RT–PCR with specific primers are identical with those of the clones isolated from the cDNA libraries, confirming that mRNA species corresponding to the two isoforms of GMAP-210 are expressed in HeLa cells.

We used the *gmap-210* cDNA sequence to perform a search of the human genome data library at NCBI with the BLAST

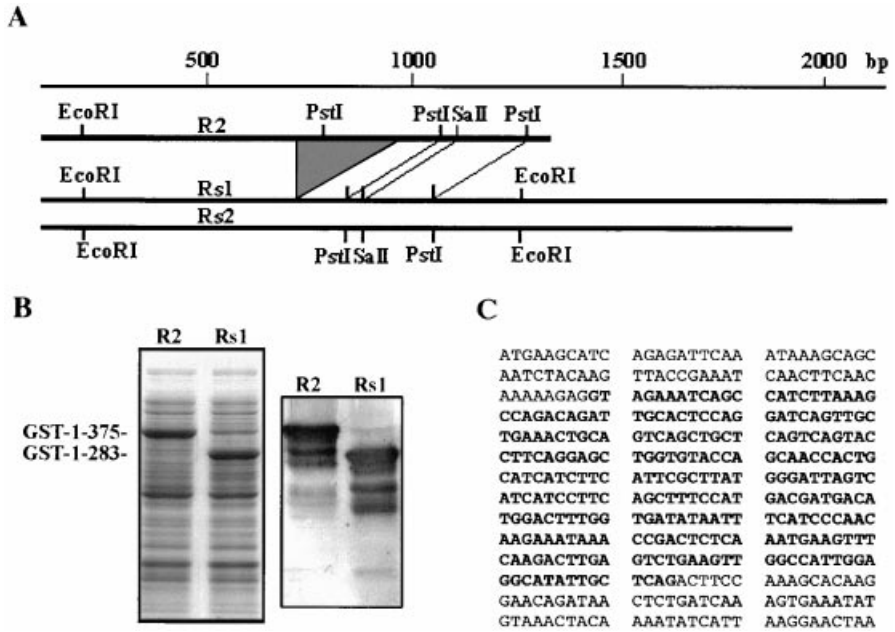

Figure 1 Analysis of clones obtained for the N-terminal region of GMAP-210 and GMAP-200

(**A**) DNA from clones R2, Rs1 and Rs2 were digested with the restriction enzymes *Eco*RI, *Eco*RI–*Pst*I and *Eco*RI–*Sal*I and analysed by electrophoresis in a 1 % (w/v) agarose gel. The deduced restriction map is shown. A fragment of approx. 0.3 kb, including a *Pst*I restriction site, is absent from Rs1 and Rs2. (**B**) Coomassie Blue staining of electrophoretically separated protein extracts from bacteria expressing the indicated GST fusion polypeptides (left panel). Samples of the same bacterial extracts were subjected to electrophoresis, transferred to a nitrocellulose membrane and blotted with RM autoimmune serum (right panel). (**C**) The DNA sequence of the region absent from Rs1 and Rs2 is shown in bold.

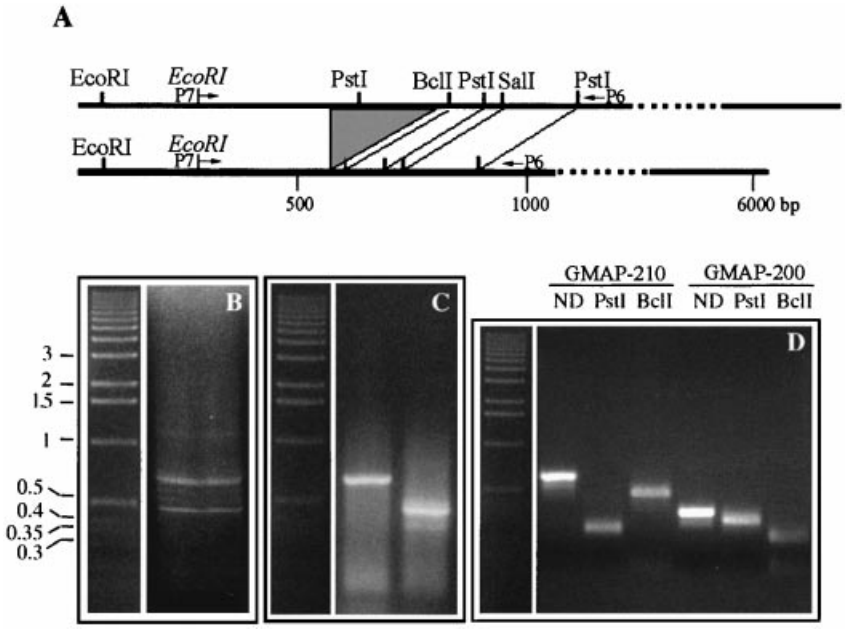

Figure 2 RT–PCR amplification of two forms of *gmap-210* mRNA

(**A**) mRNA from HeLa cells was subjected to RT–PCR with primers P7 and P6. The bands obtained (**B**) were purified from the gel, reamplified with the same primers and analysed by agarose-gel electrophoresis (**C**). The bands were digested with restriction enzymes *Pst*I and *Bc*lI (**D**) to ascertain that they corresponded to the bands expected for *gmap-210* and *gmap-200*. Abbreviation: ND, non-digested.

Table 1 Analysis of intron/exon junctions of the *gmap-210* gene

Intron sequences are in lower case and exon sequences are in capitals. The positioning of introns between codons is indicated by phase 0, interruption after the first nucleotide by phase I, and interruption after the second nucleotide by phase II. The first nucleotide of the translation initiation codon (ATG) is designated position +1. Amino acid positions refer to the long form of the protein.

Exon	Splice acceptor site	Exon size (bp)	Nucleotide positions	Amino acid positions	Splice donor site	Intron size (bp)	Intron phase
1		⩾ 495	−356–139	1–46	TGGAA/gtaacagctg	6293	I
2	tctcttgtag/CAGAA	62	140–201	47–67	CAGAG/gtaagaaaaa	7771	0
3	ttttttctag/AATGA	111	202–312	68–104	AAGAG/gtaaatgtta	3478	0
4	aaatatatag/GTAGA	276	313–588	105–196	CTCAG/gtagataaaa	3805	0
5	tctgatctag/ACTTC	69	589–657	197–219	TTAAG/gtaagtcaaa	1820	0
6	atttttaag/GAACT	166	658–823	220–274	ACAAG/gttattagtt	1118	I
7	tatgttctag/GTGGC	363	824–1187	275–395	GTCTG/gtatacagtc	2419	I
8	gtttttacag/ATGCC	41	1187–1227	396–409	ACCAG/gtaaattaat	682	0
9	attttgtag/GATAA	87	1228–1314	410–438	AAAAG/gtgggtgctg	3133	0
10	atcatttcag/GAAGA	213	1315–1527	439–509	CAAAG/gtaacactgt	1191	0
11	tttctttcag/CACAT	3030	1528–4557	510–1519	AACAG/gtgtgttctg	3307	0
12	tttccaaaag/GGCAA	141	4558–4699	1520–1566	ATGAG/gtatactttc	534	0
13	ctctacctag/GTTCA	194	4670–4893	1567–1631	GCAAG/gtaatttttt	3742	II
14	ttgtttgaag/CCATC	164	4894–5056	1632–1685	ACAAG/gtaagctcta	1439	I
15	ttctctttag/AGGAA	104	5057–5160	1686–1720	TACAG/gtaggacaaa	5425	0
16	tctttctcag/GAATG	100	5161–5260	1721–1753	ACAAA/gtaggttttt	12094	I
17	tttacaacag/ATGAG	82	5261–5342	1754–1781	GACAA/gtatgctttt	821	II
18	attttcatag/AGTCC	115	5343–5457	1782–1819	AGCAG/gtgactggac	429	0
19	aatctttcag/TTGTT	117	5458–5574	1820–1858	ATAGT/gtaagaaaca	1765	0
20	tttttcttag/TCTTT	145	5575–5719	1859–1906	TAAAG/gtaaaactag	2820	I
21	tattctttag/ATACA	377	5720–6096	1907–1979			

program. The sequence in BAC R-529H20 of the RPCI-11 library from chromosome 14 contained the entire sequence for *gmap-210*. We took advantage of this sequence to elucidate the exon/intron structure of this gene. As seen in Table 1, the *gmap-210* gene consists of 21 exons and 20 introns and spans at least 70 kb of DNA. The intron sizes range from 429 bp to 12 kb; the exon sizes range from 41 (exon 8) to 3030 bp (exon 11), although the accurate length of exon 1 is unknown. A computational analysis of the 5′-flanking region of exon 1, with the Promoter Scan [13], TSSG, TSSW, FunSiteP [14] and NNPP programs, predicts a transcription start site at position −2175 relative to the translation start site. This prediction should be taken with

```
Exon III
gttgaaaata ctttttttt ctagAATGAA AGGCTTAAGA AACTTTGTAC
TGATCTAGAA GAGAAACATG AAGCATCAGA GATTCAAATA AAGCAGCAAT
CTACAAGTTA CCGAAATCAA CTTCAACAAA AAGAGgtaaa tgttatcaca
.............................(>3kb).............................
Exon IV                                                    ⟶
gttttaaagt accttctcta aaacttggat tataaatata tagGTAGAAA
TCAGCCATCT TAAAGCCAGA CAGATTGCAC TCCAGGATCA GTTGCTGAAA
CTGCAGTCAG CTGCTCAGTC AGTACCTTCA GGAGCTGGTG TACCAGCAAC
CACTGCATCA TCTTCATTCG CTTATGGGAT TAGTCATCAT CCTTCAGCTT
TCCATGACGA TGACATGGAC TTTGGTGATA TAATTTCATC CCAACAAGAA
ATAAACCGAC TCTCAAATGA AGTTTCAAGA CTTGAGTCTG AAGTTGGCCA
TTGGAGGCAT ATTGCTCAGg tagataaaaa ttttttagag tttttgaaaa
.............................(>3kb).............................
Exon V
ttttttagag gaaaatcagt ataattattt actaattctc tttttctgat
ctagACTTCC AAAGCACAAG GAACAGATAA CTCTGATCAA AGTGAAATAT
GTAAACTACA AAATATCATT AAGgtaagtc aaattgttga ttgatgatgg
```

```
Form GMAP-210
.....NERLKKLCTDLEEKHEASEIQIKQQSTSYRNQLQQKEVEISHLKARQIALQDQLLK
LQSAAQSVPSGAGVPATTASSSFAYGISHHPSAFHDDDMDFGDIISSQQEINRLSNEVSRL
ESEVGHWRHIAQTSKAQGTDNSDQSEICKLQNIIK......

Form GMAP-200
.....NERLKKLCTDLEEKHEASEIQIKQQSTSYRNQLQQKETSKAQGTDNSDQSEICKLQ
NIIK......
```

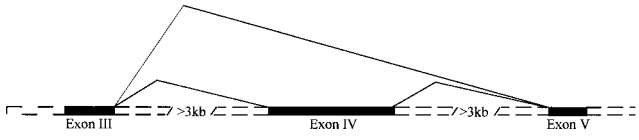

Figure 3 Alternative transcript from the human *gmap-210* gene lacks exon 4

Top panel: nucleotide sequence of exon 3, the alternative exon 4, and exon 5. Exon sequences are in capitals; flanking intron sequences are in lower case. Splice signal sequences at exon/intron boundaries are in bold. The pyrimidines near acceptor sites are underlined to show the unusual low frequency in the flanking sequence of exon 4 relative to the other exons. Middle panel: amino acid sequence of GMAP-210 and GMAP-200 isoforms in the spliced region. Exon 4 is shown in bold. Bottom panel: organization of the alternatively spliced region of the *gmap-210* gene. Exon 4 might sometimes be skipped by joining exon 3 to exon 5.

caution because only approx. 54% of the promoters are correctly recognized by the best of the above-mentioned programs. To find potential transcription binding sites, the predicted promoter region was scanned with the programs MatInspector [15] and TFSearch. This analysis identified a TATA box located at −30 nt relative to the transcription start site. In addition, many regulatory elements are predicted to bind to the putative promoter region, including GATA-1 [16], NF-Y [17], SRY [18], Nkx-2.5 [19], AP-1 [20], Sp1 [21], delta EF1 [22], TCF11 [23], Ik-2 [24], CdxA [25].

Interestingly, exon 4 corresponds exactly to the sequence of the deletion observed in cDNA clones Rs1 and Rs2, strongly suggesting that these clones arose from an alternative splicing of *gmap-210* primary transcript. Intron–exon junctions match well with the reported minimal consensus sequences (GT at the beginning of the intron and AG at the end). The reported consensus for acceptor sites [26,27] predicts a high frequency of C and T in the 5′-flanking region of the AG consensus. The average T+C content in this region for the 20 acceptor sites in *gmap-210* is 79%. However, the acceptor site located in the junction between intron 3 and exon 4 is the only one with less than 50% T+C content (43%). The hypothesis supported by these genetic data is shown in Figure 3: that the acceptor site of intron 3 might sometimes not be recognized by the spliceosome and the next acceptor site would be used instead. This mechanism could generate an isoform lacking exon 4.

As shown in Figure 4, GMAP-210 is organized into three functional domains: an N-terminal Golgi-binding domain that spans exons 1–7 (residues 1–375), a central coiled-coil domain encoded by exons 7–17 (residues 376–1778) and a C-terminal microtubule-binding domain from exons 18–21 (1779–1979). A detailed analysis of the secondary structure of the N-terminal Golgi-binding domain of GMAP-210 revealed that it consists of two acidic non-helical regions interrupted by a small coiled-coil domain and followed by a long coil. Exon 4 corresponds approximately to the second non-helical region. Therefore in the short variant of GMAP-210 the N-terminal domain contains only an acidic non-helical region and a small coiled-coil domain preceding the long coil (Figure 5A).

Because the deletion present in GMAP-200 is located inside the Golgi-binding domain (as represented in Figure 5A), we first analysed the effect of this deletion on the subcellular localization of the protein. For this purpose, full-length cDNA species coding for GMAP-210 or GMAP-200 with an N-terminal HA epitope were introduced in COS-7 cells by electroporation. The HA epitope was shown not to interfere with the association of GMAP-210 with Golgi membranes (results not shown; see [6]). Cells were incubated, fixed, double-labelled and finally observed with a immunofluorescence microscope (Figure 5B). Both proteins localized to a compact juxtanuclear reticulum characteristic of the Golgi apparatus as revealed by an anti-HA antibody (Figure 5B, left panels). The labelling pattern overlapped exactly that exhibited by RM130, a polyclonal serum that recognized both exogenous and endogenous GMAP-210 proteins (results not shown; see [6]) and mostly co-localized with that displayed by an anti-giantin monoclonal antibody (Figure 5B, right panels). These results indicate that the short form of the protein is targeted to the same place as the endogenous and exogenous GMAP-210, i.e. the Golgi membranes. In addition, GMAP-200 overexpression perturbed the Golgi apparatus in the same way as GMAP-210 overexpression; transfected cells showed a marked enlargement and partial fragmentation of the Golgi apparatus (Figure 5B; compare the transfected and non-transfected cells). As expected, overexpression of GMAP-200 had similar disruptive effects on microtubule organization as overexpression of GMAP-210 (Figure 5C). The array of microtubules in the centrosomal area appeared modified in cells overexpressing GMAP-210 (Figure 5C, middle panels) and GMAP-200 (Figure 5C, bottom panels). The microtubule aster became undefined and many microtubules seemed to emanate from the enlarged Golgi area rather than from the centrosome (compare non-transfected and transfected cells).

Although the high expression level of transfected GMAP-200 suggests that most of the molecules detected by the anti-HA antibody could be homodimers of GMAP-200, the possibility that exogenous GMAP-200 could dimerize with endogenous GMAP-210 cannot be excluded. Heterodimers between GMAP-210 and GMAP-200 could mask a particular effect of the spliced isoform when overexpressed. To test this possibility we performed co-immunoprecipitation experiments. COS-7 cells were transfected in parallel with a GFP-tagged version of GMAP-210, an HA-tagged form of GMAP-200 or both. After incubation, cells were lysed in NP40 buffer and centrifuged; supernatants were analysed by immunoblotting with an anti-(GMAP-210) antibody (RM130) to monitor transfection efficiency (Figure 5D, upper panel). Supernatants were also immunoprecipitated with an anti-HA antibody linked to Protein A–Sepharose beads. After being washed, complexes were analysed by immnoblotting with RM130 antibody. As can be seen in Figure 5(D) (lower panel), both

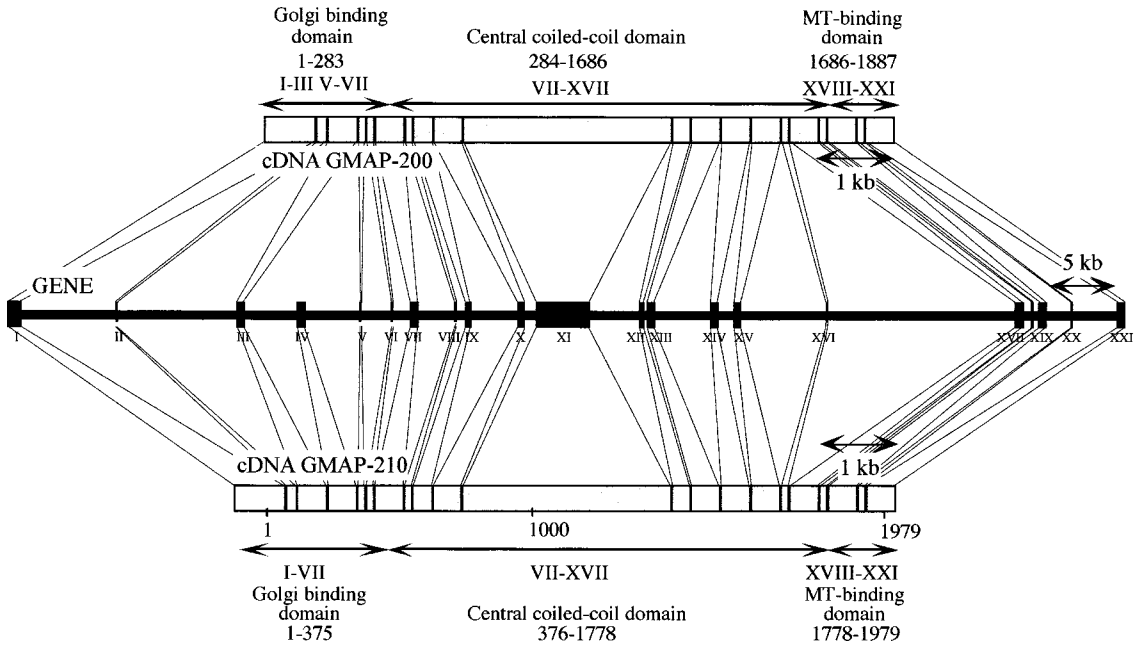

Figure 4 Physical map of human *gmap-210* gene

The cDNA of the two alternative transcripts and important functional domains of the encoded proteins are shown at the top and at the bottom. The exon–intron organization of the gene is shown in the middle. The genomic sequence used for this analysis was obtained from the National Centre for Biotechnology Information database and is included in BAC R-529H21.

isoforms were detected when immunoprecipitation was made from doubly transfected cells. Similar results were obtained when anti-GFP antibody was used for immunoprecipitation instead of anti-HA antibody (results not shown). These results indicate that both GMAP-210 and GMAP-200 are able to dimerize, at least when overexpressed, and represent the first evidence for a oligomeric state of the protein *in vivo*.

We also used cells overexpressing GMAP-210 and GMAP-200 to investigate the expression of both isoforms in normal cells by using high-resolution PAGE followed by immunoblot analysis with RM130 polyclonal serum. As shown in Figure 5(E), in non-transfected cells RM130 decorated a doublet, with a more intense upper band. Overexpression of GMAP-210 produced an increase in the amount of the upper band, whereas overexpressed GMAP-200 co-migrated with the lower band, supporting the notion that bands observed in non-transfected cells corresponded to GMAP-210 and GMAP-200. These observations, together with the isolation of two independent clones from an expression library (Rs1 and Rs2) and with the results obtained by RT–PCR (Figure 2), indicate that GMAP-200 is expressed in cells.

To examine the ability of GMAP-200 to bind to the Golgi membranes, COS-7 cells were transfected either with a truncated mutant of GMAP-210 consisting of the N-terminal Golgi-binding domain (ΔC375–GFP) or with the corresponding domain in GMAP-200 (ΔC283–GFP). Transfected cells were then homogenized and fractionated by centrifugation. Similar quantities of membrane pellets (MP) and supernatants (SP) were processed by immunoblotting with a monoclonal anti-GFP antibody (Figure 6A, top panel). Blots were analysed quantitatively by densitometry to determine the distribution of each GFP-fusion protein between the two fractions. Identical blots were revealed with RM130 and anti-(α-tubulin) antibody as controls for the correct fractionation of membranes and for loading (Figure 6A, middle and bottom panels). Membrane pellets contained most of the GMAP-210 protein, whereas tubulin was detected mainly in supernatants. As shown in Figure 6(A), a significant proportion of both GFP-fusion proteins sedimented with the membrane fraction. Quantitative analyses revealed that 46% of ΔC375–GFP associated with membranes whereas only 27% of ΔC283–GFP did so, i.e. Golgi membranes sedimented 1.8-fold more ΔC375–GFP than ΔC283–GFP molecules.

To confirm the *in vitro* results, transfected cells were also processed for GFP fluorescence and double-labelled with RM130 [which specifically recognizes endogenous GMAP-210 (Figure

Figure 5 Effect of GMAP-210 and GMAP-200 overexpression on the Golgi apparatus

(**A**) Schematic representation of the proteins used for transfection of COS-7 cells. (**B**). COS-7 cells transiently expressing HA-GMAP-210 (upper panels) or HA-GMAP-200 (lower panels) were fixed in methanol and double-labelled with rhodamine-linked anti-HA antibodies (left panels) and anti-giantin monoclonal antibody followed by fluorescein-linked anti-mouse IgG secondary antibody (right panels). The Golgi apparatus of non-transfected cells labelled with an anti-giantin antibody are indicated by arrows for comparison. For a better appreciation of the enlargement of the Golgi apparatus, the position of the nucleus is also shown. (**C**). To examine the effects of the overexpression of both isoforms (left panels) on microtubule network organization, transfected cells were double-stained for GMAP-210 isoforms and for α-tubulin (right panels). A non-transfected cell is also shown in the top panels for comparison. Note the disappearance of the microtubule aster in the Golgi area. (**D**) COS-7 cells were transfected by electroporation with GFP-GMAP-210, HA-GMAP-200 or both and, after 24 h, NP40-soluble fractions were prepared. The expression of the transfected proteins was assessed by Western blotting with RM130 serum, a polyclonal serum that recognizes both GMAP proteins (upper panel). Soluble fractions from singly and doubly transfected cells were immunoprecipitated (IP) with anti-HA antibodies linked to Protein A–Sepharose beads and the presence of GMAP-210 isoforms in immunoprecipitates was analysed by immunoblotting with RM130 polyclonal antibody (lower panel). (**E**). Finally, COS-7 cells were transfected with non-tagged versions of GMAP-210 and GMAP-200 proteins. The expression of transfected and endogenous proteins was assessed in transfected and non-transfected cells by Western blotting with RM130 serum. Scale bars, 5 μm.

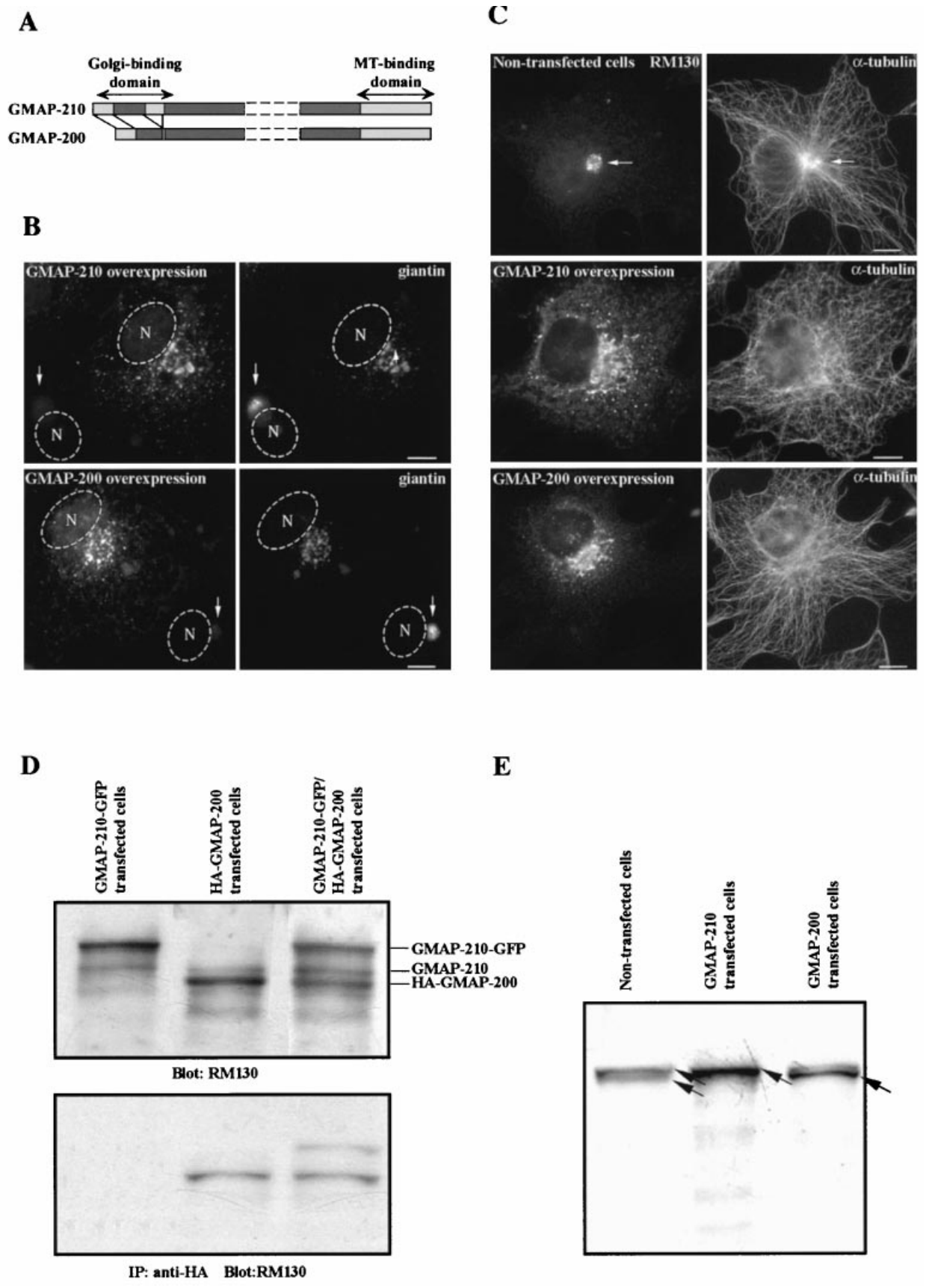

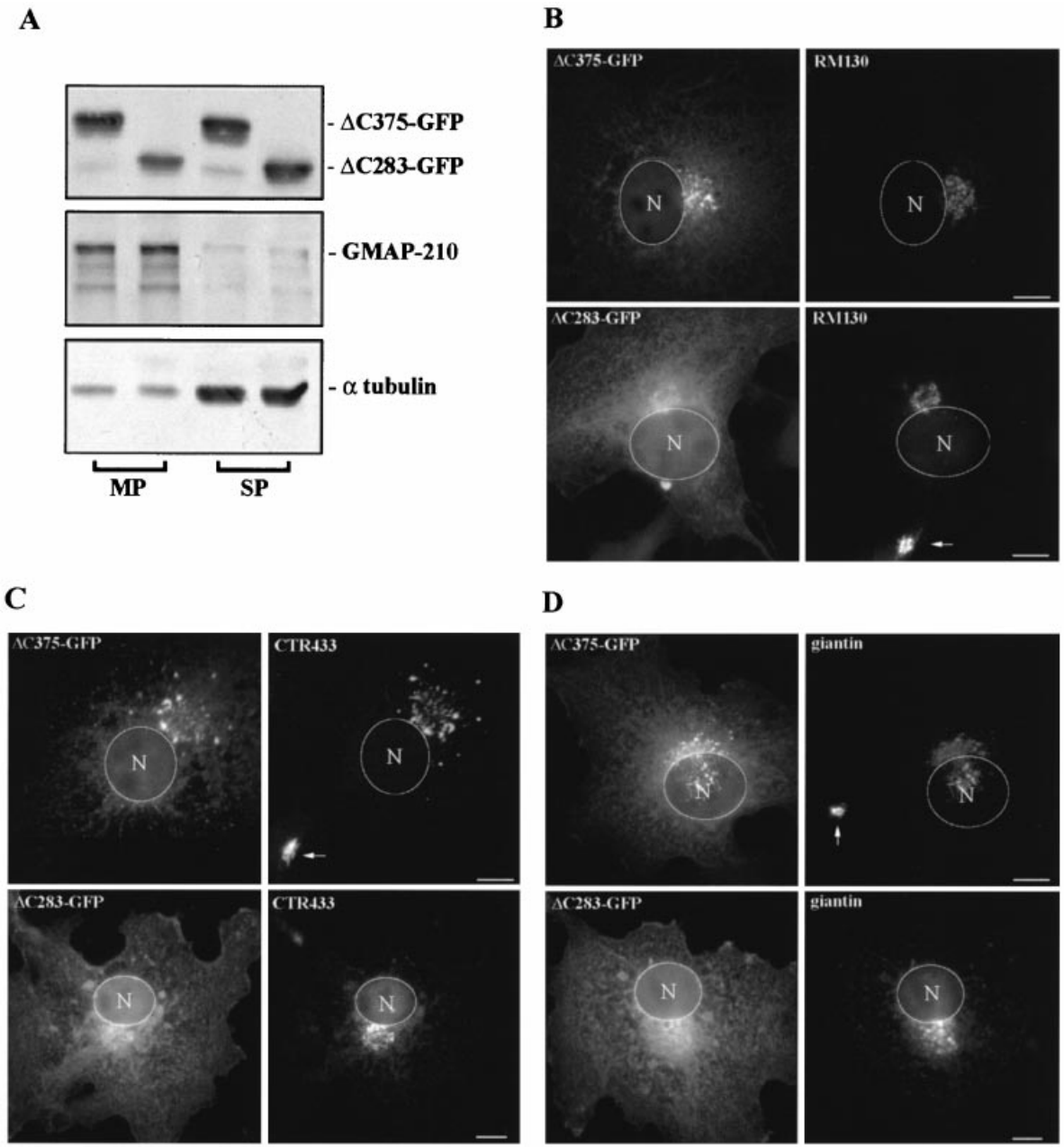

Figure 6 Transient expression of GFP-tagged N-terminal domains of GMAP-210 and GMAP-200

COS-7 cells were transfected with the truncated forms ΔC375–GFP or ΔC283–GFP corresponding to the N-terminal domains of GMAP-210 and GMAP-200 respectively (**A**). Transfected cells were mechanically disrupted and membrane-enriched fractions were obtained by centrifugation. Distribution of truncated mutants between membrane-containing pellets (MP) and supernatants (SP) was investigated by Western blotting with anti-GFP monoclonal antibody (top panel). The distributions of endogenous GMAP-210 (middle panel) and α-tubulin (bottom panel) were also determined as controls for the correct fractionation of membranes and for loading. Alternatively, transfected cells were also processed for GFP fluorescence and double-labelled with RM130 polyclonal antibody (**B**), CTR433 monoclonal antibody (**C**) or anti-giantin monoclonal antibody (**D**). Positions of the nuclei are indicated. Arrows indicate non-transfected cells. Scale bars, 5 μm.

6B)], CTR433 [a medial Golgi marker (Figure 6C)] or anti-giantin (Figure 6D) antibodies. ΔC375–GFP seemed to be cytosolic but was also localized in punctate structures clustered in the Golgi region (Figures 6B, 6C and 6D, upper panels). When ΔC283–GFP was expressed, most of the transfected cells (more than 80 %) exhibited the phenotype shown in the lower panels of Figures 6(B), 6(C) and 6(D) in that no punctate structures were seen; instead, GFP fluorescence seemed distributed throughout the cytoplasm although more concentrated in a perinuclear localization. The rest of the cells showed a labelling pattern similar to that observed in ΔC375–GFP-transfected cells. Double labelling with RM130 revealed partial co-localization, indicating that truncated mutants were able to bind to the CGN membranes. In both cases, RM130 labelling was less intense, although to different extents, when compared with a non-transfected cell (arrow in Figure 6B), suggesting that endogenous protein had been partly displaced from the membranes. Consistent with the association level of truncated forms with CGN membranes,

the effect of ΔC375–GFP on Golgi cisternae morphology was also more pronounced, as revealed by double labelling with the Golgi markers CTR433 and giantin (Figures 6C and 6D). Instead of the normal compact Golgi seen in untransfected cells, both markers appeared in some punctate structures that remained in the Golgi area. No significant changes in Golgi morphology could be seen when ΔC283–GFP was expressed (compare the upper and lower panels of Figures 6C and 6D). It must be noted that cells shown in Figure 6 expressed intermediate levels of truncated proteins. At very high expression levels, the Golgi membranes disappeared, probably by redistributing in the endoplasmic reticulum as reported previously [6], and no differences between truncated forms were found. Taken together, these results demonstrate that the N-terminus of GMAP-200 retains the capacity for interacting with Golgi membranes but more weakly (almost a half) than the homologous domain in GMAP-210.

DISCUSSION

Here we have described the isolation and characterization of an alternatively spliced GMAP-210 isoform, named GMAP-200, that originated by the deletion of exon 4. Both isoforms are expressed in COS-7 and HeLa cells, as detected by RT–PCR and immunoblot analyses. The entire sequence of *gmap-210* gene is now available in databases and consists of 21 exons and 20 introns of variable lengths. We have analysed the exon/intron junctions of the *gmap-210* gene and found that the T + C content of the junction between intron 3 and exon 4 is significantly lower than the rest. These genetic data support the hypothesis that the acceptor site of intron 3 might sometimes not be recognized by the spliceosome and the next acceptor site would be used instead, resulting in skipping of the optional exon 4 and thus in an alternatively spliced variant. Our analysis also suggests that no further alternatively spliced variants of GMAP-210 are generated by this mechanism.

Exon 4 is localized in the N-terminal domain of GMAP-210, where the capacity for membrane binding and Golgi localization resides specifically [6]. For these reasons we examined the capacity of whole GMAP-200 or a truncated mutant consisting of its N-terminal domain for binding to Golgi membranes. When overexpressed, GMAP-200 was associated with Golgi membranes and no differences in phenotype induced by GMAP-210 overexpression in both Golgi morphology and microtubule organization were visible. However, the truncated mutant displayed a lower binding capacity to Golgi membranes than the homologous domain in GMAP-210, in assays both *in vitro* and *in vivo*. Overexpression conditions and the formation of heterodimers between exogenous long and short forms of the protein, which we have demonstrated, could mask the membrane affinity differences exhibited by the truncated mutants. These heterodimers could display a higher affinity for Golgi membranes than GMAP-200 homodimers, leading to a specific enrichment of these complexes in CGN membranes.

From our results we conclude that the short form of GMAP-210 interacts more weakly with the membrane-binding sites than the full-length form. At a structural level, the loss of exon 4 decreases the N-terminal non-helical end to the first 52 residues of the protein that are now followed by a long coiled-coil fragment extending for more than half of the protein. It is tempting to speculate that the incorporation of exon 4, which disrupts the α-helix, could increase the number of GMAP-210 molecules associated with Golgi membranes, as well as the converse.

Proteins that can bind both microtubules and membranes are emerging as potentially important in stabilizing steady-state interactions between membranes and microtubules. Activities of these static linkers must be regulated to allow membrane traffic. Proteins bound to the microtubule surface might provide steric hindrance to efficient movement. In fact, overexpression of MAP4 [28] and tau [29] can inhibit organelle movement and membrane trafficking. Because proteins that act as cross-linkers are also expected to interfere with movement, it is likely that their activities are also regulated. An obvious mechanism for achieving this is the regulation of microtubule-binding capacity by phosphorylation, as has been described for CLIP-170 or MAPs [30–32]. However, other mechanisms might also be considered. GMAP-210 serves as a linker between the CGN and microtubules anchored in the centrosome. Therefore both N-terminal Golgi-binding and C-terminal microtubule-binding domains might be good targets for regulatory mechanisms. Our previous work emphasizes how modulating the number of microtubule-binding sites in the surface of the CGN membranes could be significant for ensuring the proper localization and structure of the Golgi apparatus. Excess GMAP-210 causes a local stabilization of microtubules that perturbs membrane traffic and, as a consequence, the Golgi apparatus structure. In contrast, in the absence of membrane-bound GMAP-210, the Golgi membranes become unstable [6]. The existence of a new isoform and the possibility of different oligomer formation *in vivo* provide the cell with a subtle mechanism for regulating the association of the Golgi apparatus with microtubules and consequently for ensuring the correct functioning of membrane traffic pathways.

In conclusion, the results presented here reveal the existence of a new isoform of GMAP-210 arising from alternative splicing due to the presence of an optional exon. Alternative splicing of pre-mRNA species is a powerful and versatile regulatory mechanism that can effect the quantitative control of gene expression and the functional diversification of proteins. In fact, it has been proposed as a major method of increasing physiological complexity, given the small number of human genes recently estimated [33]. In addition, it contributes to major developmental decisions and also to fine tuning of gene function [34]. We postulate that this mechanism is used for modulating the association of GMAP-210 with membranes and consequently the interaction of CGN membranes with microtubules. A more extensive analysis to improve our understanding of the different roles of these two isoforms of GMAP is currently under way.

We are indebted to Dr H. P. Hauri for kindly providing us with anti-giantin antibody, and Dr P. Chambon (Strasbourg) for the generous gift of random and oligo(dT)-primed λZAP-II libraries. This work was supported by grants from the Junta de Andalucía and from the Ministerio de Educación y Tecnología, CICYT no. PM99-0143, Spain.

REFERENCES

1 Lippincott-Schwartz, J. (1998) Cytoskeletal proteins and Golgi dynamics. Curr. Opin. Cell Biol. **10**, 52–59
2 Allan, V. J. and Schroer, T. A. (1999) Membrane motors. Curr. Opin. Cell Biol. **11**, 476–482
3 Harada, A., Takei, Y., Kanai, Y., Tanaka, Y., Nonaka, S. and Hirokawa, N. (1998) Golgi vesiculation and lysosome dispersion in cells lacking cytoplasmic dynein. J. Cell Biol. **141**, 51–59
4 Burkhardt, J. K., Echeverri, C. J., Nilsson, T. and Vallee, R. B. (1997) Overexpression of the dynamitin (p50) subunit of the dynactin complex disrupts dynein-dependent maintenance of membrane organelle distribution. J. Cell Biol. **139**, 469–484
5 Shima, D. T., Cabrera, P. N., Pepperkok, R. and Warren, G. (1998) An ordered inheritance strategy for the Golgi apparatus: visualization of mitotic disassembly reveals a role for the mitotic spindle. J. Cell Biol. **141**, 955–966

6 Infante, C., Ramos-Morales, F., Fedriani, C., Bornens, M. and Rios, R. M. (1999) A *cis*-Golgi network-associated protein is a minus end microtubule-binding protein. J. Cell Biol. **145**, 83–98

7 Rios, R. M., Tassin, A. M., Celati, C., Antony, C., Boissier, M. C., Homberg, J. C. and Bornens, M. (1994) A peripheral protein associated with the *cis*-Golgi network redistributes in the intermediate compartment upon Brefeldin A treatment. J. Cell Biol. **125**, 997–1013

8 Sambrook, J., Fritsch, E. F. and Maniatis, T. (1989) Molecular Cloning, A Laboratory Manual, 2nd edn, Cold Spring Harbor Laboratory, Cold Spring Harbor, NY

9 Wilson, I. A., Niman, H. L., Houghten, R. A., Cherenson, A. R., Connolly, M. L. and Lerner, R. A. (1984) The structure of an antigenic determinant in a protein. Cell **37**, 767–778

10 Krohne, G., Stick, R., Kleinschmidt, J. A., Moll, R., Franke, W. W. and Hausen, P. (1982) Immunolocalization of a major karyoskeletal protein in nucleoli of oocytes and somatic cells of *Xenopus laevis*. J. Cell Biol. **94**, 749–754

11 Jasmin, B. J., Cartaud, J., Bornens, M. and Changeux, J. P. (1989) Golgi apparatus in chick skeletal muscle: changes in its distribution during end plate development and after denervation. Proc. Natl. Acad. Sci. U.S.A. **86**, 7218–7222

12 Linstedt, A. D. and Hauri, H. P. (1993) Giantin, a novel conserved Golgi membrane protein containing a cytoplasmic domain of at least 350 kDa. Mol. Biol. Cell **4**, 679–693

13 Prestridge, D. S. (1995) Predicting Pol II promoter sequences using transcription factor binding sites. J. Mol. Biol. **249**, 923–932

14 Kondrakhin, Y. V., Kel, A. E., Kolchanov, N. A., Romashchenko, A. G. and Milanesi, L. (1995) Eukaryotic promoter recognition by binding sites for transcription factors. Comput. Appl. Biosci. **11**, 477–488

15 Quandt, K., Frech, K., Karas, H., Wingender, E. and Werner, T. (1995) MatInd and MatInspector: new fast and versatile tools for detection of consensus matches in nucleotide sequence data. Nucleic Acids Res. **23**, 4878–4884

16 Whyatt, D. J., deBoer, E. and Grosveld, F. (1993) The two zinc finger-like domains of GATA-1 have different DNA binding specificities. EMBO J. **12**, 4993–5005

17 Mantovani, R. (1998) A survey of 178 NF-Y binding CCAAT boxes. Nucleic Acids Res. **26**, 1135–1143

18 Harley, V. R., Lovell, B. R. and Goodfellow, P. N. (1994) Definition of a consensus DNA binding site for SRY. Nucleic Acids Res. **22**, 1500–1501

19 Chen, C. Y. and Schwartz, R. J. (1995) Identification of novel DNA binding targets and regulatory domains of a murine tinman homeodomain factor, nkx-2.5. J. Biol. Chem. **270**, 15628–15633

20 Foletta, V. C. (1996) Transcription factor AP-1, and the role of Fra-2. Immunol. Cell Biol. **74**, 121–133

21 Slansky, J. E. and Farnham, P. J. (1996) Transcriptional regulation of the dihydrofolate reductase gene. BioEssays **18**, 55–62

22 Sekido, R., Murai, K., Funahashi, J., Kamachi, Y., Fujisawa, S. A., Nabeshima, Y. and Kondoh, H. (1994) The delta-crystallin enhancer-binding protein delta EF1 is a repressor of E2-box-mediated gene activation. Mol. Cell. Biol. **14**, 5692–5700

23 Johnsen, O., Murphy, P., Prydz, H. and Kolsto, A. B. (1998) Interaction of the CNC-bZIP factor TCF11/LCR-F1/Nrf1 with MafG: binding-site selection and regulation of transcription. Nucleic Acids Res. **26**, 512–520

24 Molnar, A. and Georgopoulos, K. (1994) The Ikaros gene encodes a family of functionally diverse zinc finger DNA-binding proteins. Mol. Cell. Biol. **14**, 8292–8303

25 Margalit, Y., Yarus, S., Shapira, E., Gruenbaum, Y. and Fainsod, A. (1993) Isolation and characterization of target sequences of the chicken CdxA homeobox gene. Nucleic Acids Res. **21**, 4915–4922

26 Solovyev, V. V., Salamov, A. A. and Lawrence, C. B. (1994) Predicting internal exons by oligonucleotide composition and discriminant analysis of spliceable open reading frames. Nucleic Acids Res. **22**, 5156–5163

27 Guigo, R., Knudsen, S., Drake, N. and Smith, T. (1992) Prediction of gene structure. J. Mol. Biol. **226**, 141–157

28 Bulinski, J. C., McGraw, T. E., Gruber, D., Nguyen, H. L. and Sheetz, M. P. (1997) Overexpression of MAP4 inhibits organelle motility and trafficking in vivo. J. Cell Sci. **110**, 3055–3064

29 Ebneth, A., Godemann, R., Stamer, K., Illenberger, S., Trinczek, B. and Mandelkow, E. (1998) Overexpression of tau protein inhibits kinesin-dependent trafficking of vesicles, mitochondria, and endoplasmic reticulum: implications for Alzheimer's disease. J. Cell Biol. **143**, 777–794

30 Rickard, J. E. and Kreis, T. E. (1996) CLIPS for organelle–microtubule interactions. Trends Cell Biol. **6**, 178–183

31 Lopez, L. A. and Sheetz, M. P. (1995) A microtubule-associated protein (MAP2) kinase restores microtubule motility in embryonic brain. J. Biol. Chem. **270**, 12511–12517

32 Kitazawa, H., Iida, J., Uchida, A., Haino, F. K., Itoh, T. J., Hotani, H., Ookata, K., Murofushi, H., Bulinski, J. C., Kishimoto, T. and Hisanaga, S. (2000) Ser787 in the proline-rich region of human MAP4 is a critical phosphorylation site that reduces its activity to promote tubulin polymerization. Cell Struct. Funct. **25**, 33–39

33 Ewing, B. and Green, P. (2000) Analysis of expressed sequence tags indicates 35,000 human genes. Nat. Genet. **25**, 232–234

34 Lopez, A. J. (1998) Alternative splicing of pre-mRNA: developmental consequences and mechanisms of regulation. Annu. Rev. Genet. **32**, 279–305

Received 16 March 2001/30 April 2001; accepted 30 May 2001